

BlockEmulator: An Emulator Enabling to Test Blockchain Sharding Protocols

Huawei Huang , Senior Member, IEEE, Guang Ye, Qinde Chen, Zhaokang Yin, Xiaofei Luo, Jianru Lin, Taotao Li, Qinglin Yang , Zibin Zheng , Fellow, IEEE

Abstract—Numerous blockchain simulators have been proposed to allow researchers to simulate mainstream blockchains. However, we have not yet found a testbed that enables researchers to develop and evaluate their new consensus algorithms or new protocols for blockchain sharding systems. To fill this gap, we developed BlockEmulator, which is designed as an experimental platform, particularly for emulating blockchain sharding mechanisms. BlockEmulator adopts a lightweight blockchain architecture so developers can only focus on implementing their new protocols or mechanisms. Using layered modules and useful programming interfaces offered by BlockEmulator, researchers can implement a new protocol with minimum effort. Through experiments, we test various functionalities of BlockEmulator in two steps. Firstly, we prove the correctness of the emulation results yielded by BlockEmulator by comparing the theoretical analysis with the observed experiment results. Secondly, other experimental results demonstrate that BlockEmulator can facilitate measuring a series of metrics, including throughput, transaction confirmation latency, cross-shard transaction ratio, the queuing status of transaction pools, workload distribution across blockchain shards, etc. We have made BlockEmulator open-source in Github.

Index Terms—Blockchain, Testbed, Consensus Protocol, Blockchain Sharding

I. INTRODUCTION

Blockchain researchers need an experimental tool to verify the correctness or test the performance of their proposed protocols and algorithms. A handful of blockchain simulators have been proposed in the literature for different aims. For example, BLOCKBENCH [1] is designed for simulating and analyzing the performance of private blockchains. VIBES [2] enables blockchain simulation in large-scale network topologies and offers powerful visualization tools. SimBlock [3] is an event-driven simulator, which is suitable for studying the effect of block propagation in blockchain networks. Other simulators (e.g., Ganache [4], EthereumJS TestRPC [5], Parity Ethereum [6], the built-in emulator of Hyperledger Fabric [7], and Corda [8]) focus on simulating the fundamental functions of a blockchain such as smart contracts and transactions.

On the other hand, we find that the experiments of existing blockchain publications are mostly conducted through simulations. Their simulations must be implemented by building

This work was partially supported by the National Key R&D Program of China (No. 2022YFB2702304), NSFC (No. 62272496, No. 62032025), and Fundamental Research Funds for the Central Universities, Sun Yat-sen University (No. 231gjbj019).

All authors are with Sun Yat-Sen University, China.

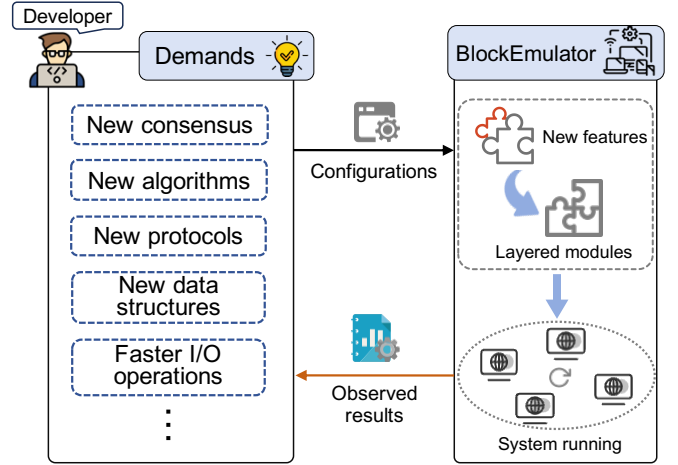


Fig. 1: The design principle of *BlockEmulator*.

a new blockchain or using existing blockchains [9]–[11]. However, building a new blockchain from scratch requires many efforts, thus consuming a lot of time, not to mention designing new protocols on top of their new blockchain. Existing blockchains like Ethereum [12] have a vast codebase, making them impractical for designing new consensus protocols. For instance, it is challenging to design blockchain-sharding protocols on top of Ethereum, let alone re-designing other underlying layers, such as the storage and data layers. In addition, in the scenarios where researchers seek to verify their protocols and algorithms, they aim to implement these solutions rapidly. They also need to initiate a testing platform and collect experimental data for performance evaluation.

Although these existing open-source simulation codes [9]–[11] have their merits, they are incapable of supporting the demands of verifying new consensus protocols related to blockchain-sharding mechanisms. This is because a blockchain sharding system is complicated. It requires not only the design of intra-shard consensus but also the organization policy of shard committees, inter-shard consensus algorithms, cross-shard communication mechanisms, the security guarantee for blockchain shards, and the atomicity of executing cross-shard transactions, etc. Thus, implementing a blockchain-sharding mechanism is usually tailored when designing a particular consensus algorithm for the sharded blockchain. When researchers change their research focus, they must implement another new blockchain sharding simulation framework as their experiment tool.

A better approach for blockchain researchers is to use a well-designed experiment platform that enables them to create new features of blockchain sharding with minimum effort. To design an experimental tool that supports sharding mechanisms, it is necessary to determine the layered architecture of the sharded blockchain and develop the required components accordingly. Each component should also provide sufficient interfaces so that users can conveniently design new mechanisms without worrying about the code’s cross-layer operations. For example, S-Store [13] enables a dedicated data structure for the storage migration of shard data. If deploying a blockchain on S-Store, the focus would be mainly on implementing the underlying database interfaces of the blockchain and making minimal modifications to other layer data structures. Similarly, when deploying asynchronous BFT consensus algorithms on blockchain shards using Dispersedledger [14], users would only require modifying the consensus layer within each shard. In addition, to deploy account redistribution algorithms [15], users only need to modify partial communication mechanisms among shards in the consensus layer of Dispersedledger. Therefore, implementing an experimental platform for blockchain sharding mechanisms involves multiple functionalities such as state management, cross-shard transactions, data availability, and inter-shard consensus. Hence, developing an effective experimental tool for blockchain sharding presents the following challenges.

- **Modular architecture.** The tool requires a modular architecture to facilitate development across various layers of the blockchain system. This design ensures both flexibility and adaptability for different use cases.
- **Interfaces for customized implementations.** The platform must provide diverse interfaces to support the development of complex sharding consensus protocols. It must also enable the measurement of various performance metrics.
- **Result accuracy.** Ensuring the correctness of experimental results is critical, as it directly affects the validity of research findings and the tool’s reliability.

However, we have not yet found such an experimental tool in the literature. To fill this gap, we design a lightweight experimental platform named *BlockEmulator*, which enables researchers to develop and test new blockchain sharding protocols. As depicted in Fig. 1, BlockEmulator only implements the core functions of a blockchain system, including node manager, consensus module, and on-chain transaction storage. For example, a client only has to configure the experimental parameters of BlockEmulator according to his/her design. After performing emulation, researchers can collect the experimental results from log files.

BlockEmulator also includes popular consensus protocols that can be utilized in sharded blockchains, such as Proof-of-Work (PoW) and Practical Byzantine Fault Tolerance (PBFT). In particular, BlockEmulator offers the system-level design and implementation of blockchain sharding mechanisms. The handling of cross-shard transactions implemented in BlockEmulator includes the following two representative solutions, i.e., *transaction relaying mechanism* proposed by Monoxide [16]

and *BrokerChain* protocol [17].

The contributions of this paper are summarized as follows.

- BlockEmulator is designed as an open-source experimental tool for evaluating blockchain sharding protocols. It provides a modular architecture design and rich interfaces that enable researchers to quickly implement their customized new algorithms, protocols, and mechanisms. It also offers useful functions for researchers to help them collect various experimental metrics.
- We designed experiments to show the correctness of BlockEmulator. Experimental results demonstrate that BlockEmulator can measure various metrics of a sharded blockchain, including transaction throughput, transaction confirmation latency, the queueing status of transaction pools, cross-shard transaction ratio, workload distribution across blockchain shards, etc.
- BlockEmulator has attracted an initial group of users from GitHub [18].

The remainder of this paper is organized as follows. Section II is a background on PBFT, Sharding Mechanisms, and the Testing Environments of Existing Blockchain. Section III provides preliminaries and analysis of the cross-shard mechanism. Section IV presents the module design and framework of BlockEmulator with details. Section V conducts extensive experiments to verify the functional performance of BlockEmulator. Finally, Section VI concludes this work.

II. BACKGROUND

In this Section, we introduce the background of the proposed BlockEmulator, including the PBFT consensus protocol, sharding mechanisms, and existing representative blockchain experiment tools.

A. Practical Byzantine Fault Tolerance

PBFT [19] is a classic Byzantine fault-tolerant algorithm. Byzantine faults refer to those nodes that may send incorrect messages, tampered messages, or not send messages at all. PBFT guarantees that the system is still able to achieve consensus even when a certain number of Byzantine nodes exist in the system. This algorithm is widely used in mainstream blockchain systems such as consortium blockchains. For each consensus round, the main idea of PBFT is to select a primary node as the leader node, which is responsible for receiving and pre-processing requests from clients. When a proposal (e.g., a new block) is ready, the leader node broadcasts the proposal to other nodes. The other nodes decide whether to accept the proposal through voting. Once a certain number of nodes achieve a consensus, the proposal is confirmed. Then, this confirmed message proceeds to the next step of broadcasting. After going through the per-preparing, preparing, and committing phases, nodes achieve consensus and execute all transactions included in this confirmed proposal. Upon completing the execution of all transactions, the PBFT protocol sends a receipt message to clients. This round of PBFT finishes.

B. Blockchain Sharding

Sharding technique divides a single blockchain into multiple parallel smaller blockchain shards to achieve scalability. Each blockchain shard is only responsible for maintaining the account state of a subset of transactions. Thus, the sharding mechanism can improve the throughput of the entire blockchain system.

Blockchain sharding can be classified into three categories, i.e., network sharding, transaction sharding, and state sharding. Among them, state sharding has become the research focus due to its low storage requirements [16], [17]. Following the static state sharding approach, if a proof-of-work (PoW) blockchain is segmented into $S > 0$ shards, the blockchain's performance has the potential to be scaled out by a factor of S . However, the computational power of the blockchain system will be distributed across all shards. Such the segmentation of consensus power reduces the security level to $1/S$. Malicious nodes would make it easier to attack a specific shard with their consensus power. This is because there will always be a shard with computational power less than or equal to $1/S$, according to the pigeonhole principle [20]. Sacrificing a significant amount of security for higher throughput is not acceptable for a blockchain system. Therefore, the design of security mechanisms for blockchain sharding systems is crucial.

In blockchain systems that adopt the account/balance model, Monoxide [16] is a representative solution. The ‘‘Chu-ko-nu Mining’’ consensus proposed by Monoxide ensures that the security of the blockchain system does not decrease as the number of shards increases. All shards in Monoxide perform PoW consensus protocol simultaneously. Unlike the static state sharding algorithm, each shard's PoW can be added to other shards' local chains as long as it meets the mining difficulty. Through this approach, the effective computational power within each shard is amplified by a factor of S (i.e., the number of shards). This feature ensures the system's security. Monoxide adopts the address partitioning policy by the address's suffix, aiming to prevent malicious nodes from intentionally concentrating in one specific shard.

In state sharding that adopts the account/balance-based transaction model, the blockchain system can be described as a structure consisting of a final committee and several worker shards. The final committee is also called the *main* shard. In such cases, the blockchain system usually combines multiple mechanisms rather than relying on a single pure consensus mechanism. Committee members are periodically elected using more secure mechanisms like PoW to prevent Sybil attacks [21] and bribery attacks [22]. *Worker* shards generally employ high-throughput consensus mechanisms like PBFT for block generation to improve the system's throughput. The main shard is responsible for various configurations and adjustments that benefit the performance of the blockchain. For example, the main shard makes periodic reconfiguration to the blockchain sharding system. The performance of the sharded blockchain system is mainly provided by the *worker* shards. While running, the blockchain sharding system goes to the next consecutive epoch when a specific running time

expires or after a predefined number of blocks are generated. A reconfiguration phase will be executed before the next epoch begins.

C. Representative Blockchain Experiment Tools

Through a thorough literature review, we have found the following representative simulators, emulators, or platforms that can be adopted as experiment tools for blockchain researchers.

- Ganache [4], formerly called TestRPC, is a blockchain emulator developed by Truffle Suite. It provides a local blockchain environment that allows developers to simulate Ethereum networks. Ganache supports features like smart contract development, transaction simulation, and account management.
- EthereumJS TestRPC [5] is a *Nod.js*-based emulator that provides a local Ethereum blockchain for testing and development purposes. It offers a lightweight and configurable environment for running test codes and deploying smart contracts.
- Parity Ethereum [6] provides a fully functional environment with mining capabilities, account management, and smart contract deployment. It enables developers to create a local private blockchain for testing Ethereum applications.
- Hyperledger Fabric [7] is a permissioned blockchain platform, which provides a built-in emulator for testing smart contracts and applications. It provides a local development environment that allows developers to simulate a blockchain network, create and interact with channels, deploy and invoke chain codes, and test consensus mechanisms.
- Corda [8] is a blockchain platform designed for enterprise, including a mock network feature that allows developers to emulate a Corda network for testing and development. The mock network provides a simulated environment to deploy and test Corda contracts, flows, and transactions.

Given the existing experiment tools, we can find that these efforts mainly focus on the functions of smart contracts and transaction executions. Nevertheless, we have not found a dedicated emulator that offers blockchain-sharding mechanisms and the handling of cross-shard transactions.

III. PRELIMINARIES OF BLOCKCHAIN SHARDING

In this section, we elaborate on the preliminaries of blockchain sharding mechanisms, including the terminologies, concepts, and critical issues of blockchain sharding.

A. Cross-Shard Transactions

As shown in Fig. 2, suppose that there are three accounts A , B , and C , and two blockchain shards. Accounts B and C locate at Shard #2, while Account A locates at Shard #1. Thus, the transaction ($C \rightarrow B : x$) is called a *regular* TX, which will be handled only in Shard #2. In contrast, the transaction ($A \rightarrow B : y$) becomes a *cross-shard* TX.

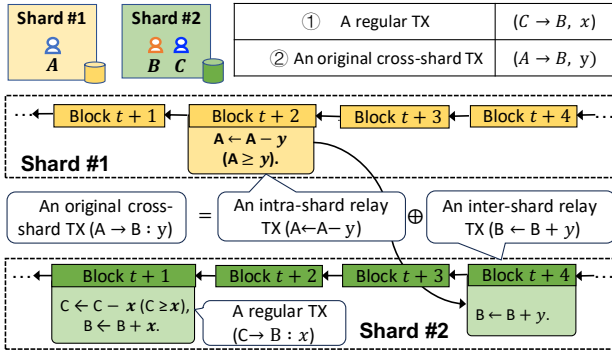


Fig. 2: The illustration of multiple types of transactions, including a regular transaction, an original cross-shard transaction, an intra-shard relay transaction, and an inter-shard relay transaction.

Monoxide [16] divides an original cross-shard transaction ($A \rightarrow B : y$) into an *intra-shard* relay transaction ($A \leftarrow A - y$) and an *inter-shard* relay transaction ($B \leftarrow B + y$), aiming to achieve the so-called *eventual atomicity* of a cross-shard transaction. The intra-shard relay transaction deducts the funds from the payer’s account in the source shard, while the inter-shard relay transaction deposits the funds into the payee’s account in the destination shard. These two relay transactions are connected through transaction-relaying messages.

While handling all transactions in each shard, miners select transactions from the local transaction pool (abbr. as TX pool) to generate a new block. These miners can interpret whether an original transaction in the block is a cross-shard transaction (abbr. as CTX) or an intra-shard regular transaction according to the locations of the payer and payee accounts. That is, the inter-shard relay transaction of the original CTX will be relayed to the payee’s shard (i.e., the destination shard) after the block is committed on the payer’s shard local chain. Once a consensus node receives an inter-shard relay transaction, it will check whether the related intra-shard relay transaction has been successfully included in the blockchain ledger. If the corresponding intra-shard relay transaction is on the chain, this consensus node adds the inter-shard relay transactions to its TX pool for future packaging.

As shown in Table I and Fig. 2, to better understand the correlations between inside-shard and cross-shard transactions in a sharded blockchain, we let $\mathcal{U}, \mathcal{V}, \mathcal{W}, \mathcal{X}, \mathcal{Y}, \mathcal{Z}$ denote the set of inter-shard relay transactions, intra-shard relay transactions, transactions packed into all historical blocks, all historical transactions submitted to TX pools by TX payers, all historical cross-shard transactions, and all historical regular transactions, respectively. Note that, all those non-cross-shard transactions are the *regular transactions*, which can be handled easily by the local consensus within a particular shard. Meanwhile, $|\mathcal{X}|$ represents the size of \mathcal{X} , and the same meaning applies to other symbols.

Based on the description aforementioned, we have

$$|\mathcal{Y}| = |\mathcal{U}| = |\mathcal{V}|. \quad (1)$$

A cross-shard transaction is divided into two relay transac-

TABLE I: Symbols defined for Transaction Types.

\mathcal{U}	The set of all inter-shard relay TXs
\mathcal{V}	The set of all intra-shard relay TXs
\mathcal{W}	The set of all TXs packed in historical blocks
\mathcal{X}	The set of all historical TXs submitted to TX pools by TX payers
\mathcal{Y}	The set of all historical cross-shard TXs
\mathcal{Z}	The set of all historical regular TXs

tions and will be included in two blocks eventually, we thus have the following equation.

$$\begin{cases} |\mathcal{Z}| + |\mathcal{Y}| = |\mathcal{X}|, \\ |\mathcal{Z}| + 2 \cdot |\mathcal{Y}| = |\mathcal{W}|. \end{cases} \quad (2)$$

With $|\mathcal{Y}| = |\mathcal{W}| - |\mathcal{X}|$ increasing, the number of transactions packed in the blockchain will be significantly greater than the processed transactions in practice. Thus, a sharding blockchain suffers from high latency and low throughput due to the cross-shard coordination.

B. Shard Workload Balance

Monoxide [16] allocates accounts into designated shards based on these accounts’ suffixes. However, as demonstrated in [17], some accounts could be very active and thus result in unbalanced workloads across shards. Monoxide neither considers how to reduce the proportion of CTXs nor how to balance shard workloads.

To the best of our knowledge, we have found two representative algorithms that can achieve workload balance for blockchain shards, i.e., CLPA [15] and BrokerChain [17]. They are introduced as follows.

CLPA [15] is a dynamic account allocation algorithm that is different from the static policy defined in Monoxide [16]. It can balance the workloads across shards and reduce the number of cross-shard transactions, simultaneously. In [15], committee nodes need to be selected by PoW at the beginning of each epoch. The committee then listens to newly generated blocks from each shard and generates a graph of accounts according to these new blocks. In this graph, edges are the transactions enclosed in the blocks and vertexes are the accounts associated with these transactions. When an epoch expires, the committee runs CLPA, which then returns the account reallocation results. The account graph is updated each epoch so that the workload balance across shards can be achieved by invoking graph partition algorithms such as Metis or the community-aware graph partition algorithm.

Huang *et al.* [17] proposed the BrokerChain protocol, aiming to reduce the number of cross-shard TXs. BrokerChain selects some particular accounts as *broker accounts*, each of which is duplicated in multiple shards. A CTX is transferred into two intra-shard regular transactions in BrokerChain protocol. Those two regular TXs can be quickly handled in the payer’s and payee’s shards, respectively. The quantity of transferred tokens of the original CTX is *bridged* by one specific broker account. Note that, if the payer or payee of

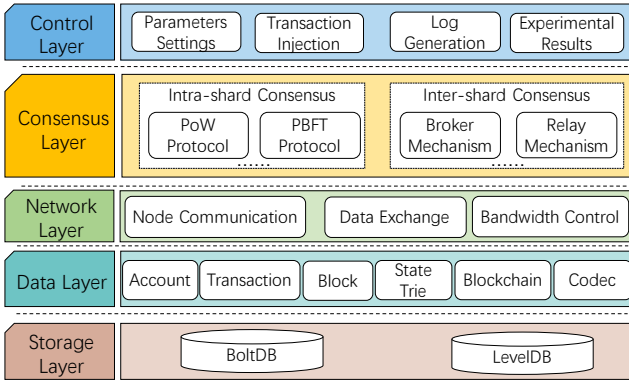


Fig. 3: The layered architecture of *BlockEmulator*.

a CTX is a broker account, this CTX becomes a regular transaction essentially. That is why BrokerChain can reduce the number of CTXs significantly.

C. The Composition of Sharding Consensus

In most blockchain sharding studies [15], [17], [23], [24], a sharding consensus protocols are composed of *worker* shards and *main* shard (i.e., the final committee). *Worker* shards are responsible for packaging blocks and achieving local consensus, while the *main* shard executes reconfiguration algorithms (e.g., CLPA [15]) and feeds back the results to the *worker* shards.

IV. DESIGN AND IMPLEMENTATION OF BLOCKEMULATOR

In this section, we elaborate on the design and implementation of *BlockEmulator*.

A. Layered Architecture

Fig. 3 shows the overview of the layered architecture of *BlockEmulator*, which consists of *Storage Layer*, *Data Layer*, *Network Layer*, *Consensus Layer*, and *Control Layer*.

1) *Storage Layer*: The storage layer stores ledger data on the disk, including the generated blockchain data, log files generated when conducting experiments, etc. For instance, consensus nodes save the confirmed blocks, transactions, account states, and system logs. The storage layer's functionality is implemented based on boltDB and levelDB. Particularly, we adopt the Merkle Patricia Tree (MPT) on top of levelDB, towards a more efficient I/O operation.

2) *Data Layer*: The data layer establishes fundamental structures of data within the system, including accounts, transactions, blocks, state trees, and nodes. The data layer interacts with the storage layer. When running *BlockEmulator*, new blocks are continually generated and encoded through the data layer. These new blocks trigger the modifications of state trees. These new tree nodes in state trees are encoded locally. The encoded blocks and account states can be stored in local files via invoking the interfaces of the storage layer. Furthermore, when an experiment is completed, the block data stored in files can be retrieved through the storage layer. The retrieved block data can be then decoded back into blocks by

the data layer. Similarly, the retrieved root nodes of state trees in different blocks can be used to generate the state trees locally. This way enables researchers to access the generated blocks and account state trees. Thus, users can examine account states offline if they are curious about the correctness of transaction execution results yielded by *BlockEmulator*.

3) *Network Layer*: The network layer is designed to support the communication across consensus nodes deployed in diverse devices. An end-to-end packet transmission mechanism is implemented by TCP, aiming to exchange data among nodes. The data exchanged includes transactions, blocks, consensus messages, etc. We implement the TCP as a keep-alive connection manner to facilitate a substantial amount of message exchanges within the network. In this manner, the TCP connection between two nodes is initiated and closed only once during the overall emulation.

4) *Consensus Layer*: The consensus layer is responsible for enabling consensus nodes to reach an agreement on a new block. In a sharded blockchain, nodes are running both the intra-shard and inter-shard consensus mechanisms. The intra-shard consensus mechanisms (like PoW and PBFT) ensure transaction consensus within a shard. The inter-shard mechanisms guarantee communication across shards. For example, to handle a CTX, the nodes located at the payer's and payee's shards should receive messages from other shards.

5) *Control Layer*: The control layer is in charge of the system execution. Before an experiment gets started, this layer needs to make preparations for configuring the experiment's environment. Preparing the experiment's environment includes initializing metric testing threads, starting listening to messages, determining the host of each consensus node, etc. When *BlockEmulator* is running, the control layer injects transactions to the transaction pools of shards at a predefined rate. The transactions injected into *BlockEmulator* can be retrieved from the historical transactions of any blockchain such as Ethereum. This layer also records the information of blocks generated by shards and the information includes not only the blocks themselves but also the necessary details of shards. When *BlockEmulator* finishes running an experiment, users can collect the experimental results from logs for scientific analysis.

B. Major Roles in BlockEmulator

As shown in Fig. 4, there are 2 types of nodes in *BlockEmulator*, i.e., *worker* nodes and *supervisor* nodes. A *worker* is responsible for packing transactions and generating blocks for the blockchain in each local shard. *Supervisor* nodes conduct global control behaviors, e.g., injecting transactions to shards, collecting committed blocks, and calculating system metrics. Note that, the number of required worker and supervisor nodes is determined by the blockchain network scale. The number of these two types of nodes can be configured flexibly according to the developer's budget.

The behaviors of *supervisors* are executed concurrently. Different *supervisors* could commit different behaviors collaboratively. However, this multiple-supervisor implementation leads to the high complexity of the emulation system. To

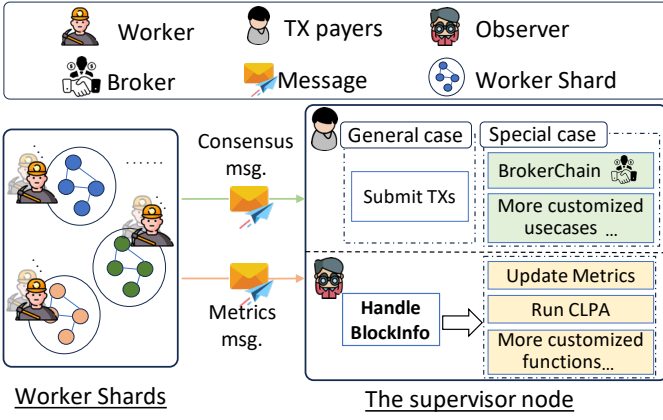


Fig. 4: Major roles of BlockEmulator, and the interactions between *worker shards* and the *supervisor node*.

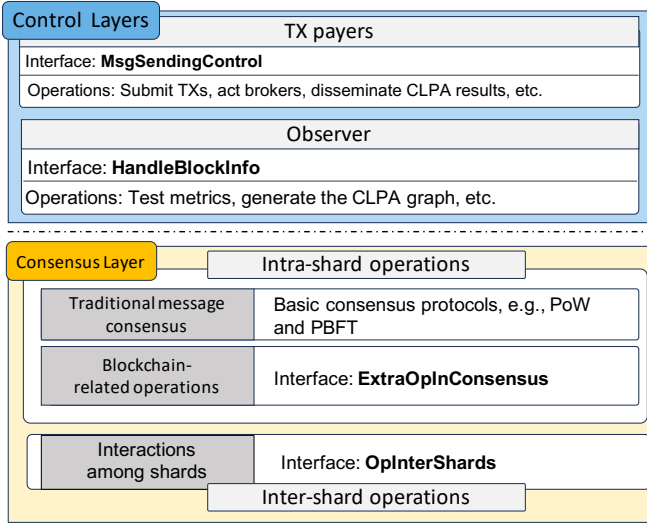


Fig. 5: The interfaces designed for Consensus Layer and Control Layer.

simplify *BlockEmulator*, we implement two roles, i.e., *TX payers* and *observer*. The first role takes on the responsibility of injecting transactions into the TX pool of each shard. As the second role, *observer* not only monitors the execution status of the blockchain system but also computes and records experimental outcomes.

Note that, in the real blockchains, there indeed are transaction payers who initiate transactions and observers who collect blocks. Accordingly, we consider these roles and add more features to them in our *BlockEmulator*. Both the *TX payers* and the *observer* can extend additional functionalities by invoking the interfaces presented in Section IV-C.

C. Core Interface Modules

To alleviate the difficulty of secondary development using *BlockEmulator*, we not only implement some of the existing popular blockchain mechanisms as pre-installed modules but also design some application programming interfaces (APIs) to meet the compatibility among mechanisms. We show primary APIs in Fig. 5. We believe that users can easily implement new

mechanisms with a few codes using the following interfaces we provide.

1) *The Intra-shard Interface in Consensus Layer*: In general, the consensus operations in a blockchain can be roughly classified into two categories: *traditional message consensus* and *blockchain-related operations*.

For example, PoW mechanism was born earlier than the blockchain as a mechanism to protect against spam emails originally [25]. In other words, PoW is a traditional message consensus and can be used in other distributed systems. However, in a blockchain environment, the PoW mechanism needs to do more operations related to blockchain, such as packing transactions, checking the correctness of all transactions enclosed in a block, and adding a new block to the blockchain.

Likewise, by incorporating blockchain-related operations, the traditional PBFT protocol can work in blockchain systems. Therefore, the details of these operations could be different across blockchains. Users should focus on their needs when designing new mechanisms on top of *BlockEmulator*. The traditional message consensus part can be easily reused because it does not need to be modified in most scenarios.

According to the analysis depicted above, we separate the *traditional message consensus* from *blockchain-related operations* in our implementation. We first design the interface **ExtraOpInConsensus** within the consensus layer to enable *blockchain-related operations*. These interfaces are then named according to their relevant functionalities, including `op_mining`, `op_verification`, and `op_confirmation`. Here, `op_mining` occurs during the message-generation phase, `op_verification` takes place during the consensus phase, and `op_confirmation` happens when consensus is achieved.

For instance, to deploy an account-migration protocol in *BlockEmulator*, the interface *ExtraOpInConsensus* can be written per the following three steps. Step i). In the account-migration protocol, the associated account states are transferred from one shard to another. To facilitate this process, during the *mining* phase, the block generator proposes either a normal block containing only TXs or a special block encompassing the account states to be migrated. Thus the method `op_mining` should be re-implemented to support two block types. Step ii). When receiving the special block, worker nodes should validate the proofs of the account states in the block. Worker nodes can accurately perform the validation by updating the function `op_verification`. Step iii). When a specific block is committed, all account states contained in the block are migrated. Then, worker nodes must update the state trie with the latest migrated account states. Consequently, the method `op_confirmation` should be modified to achieve this functionality.

Through these modifications of interface *ExtraOpInConsensus*, worker nodes can effectively handle intra-shard consensus for account migration.

2) *The Inter-shard Interface in Consensus Layer*: In a sharded blockchain, a shard must interact with other shards to synchronize some necessary information. However, the traditional consensus, such as PoW and PBFT, do not provide such

functionality. To solve this problem while enabling secondary development, we enclose the **OpInterShards** as an interface, which can help users design the rules of message handling and broadcast them across shards.

We continue to use account migration to introduce the implementation of interface *OpInterShards*, including the following two steps. Step i). Worker nodes process the account partition messages that contain information about those accounts designated for migration to different shards. Worker nodes retrieve the relevant account states from their state tries, consolidate these states into account-migration messages, and send these messages to their corresponding destination shards. By implementing the method `handleInterShardMsg` for handling account partition messages in the interface *OpInterShards*, worker nodes can accurately send account-migration messages. Step ii). When receiving the account migration message, worker nodes determine if the account states in the message are destined for their shards. Once all required account states are collected, worker nodes in those source shards are triggered to propose a special block as detailed in Sec. IV-C1. To ensure the accuracy of account migration, both the message handling and the trigger functions must be implemented in this interface effectively.

3) *Interfaces in Control Layer*: Recall that, in Section IV-B, the *supervisor* nodes play two roles (*TX payers* and *observer*) in the control layer. In practice, these two roles can be merged in only one *supervisor*, we thus implement one *supervisor* in the current version of *BlockEmulator*.

As illustrated in Fig. 4 and Fig. 5, we present two major interfaces of the *supervisor*. With these 2 interfaces, users can extend more features in *supervisor* according to their demands. We explain the functions of these two interfaces as follows.

MsgSendingControl Interface. Although the primary role of *TX payers* is to submit transactions, the interface *MsgSendingControl* provides a mechanism to allow users to extend their application purposes. For example, during the execution of an account redistribution algorithm within the blockchain, the functionality of *TX payers* can be extended through the rewriting of the interface *MsgSendingControl*. This rewriting enables *TX payers* to disseminate the updated account-partition results to worker shards. For another example, when users implement BrokerChain protocol [17], *TX payers* can play the *broker* account’s role as the transaction bridge between shards. The interface *MsgSendingControl* enables the *supervisor* node the proactive message transmission, driven by data inputs such as TXs and account partition results. This is why we refer to the role associated with this interface as the *TX payer*. This is because a TX payer acts as an active request sender in a real-world blockchain network.

HandleBlockInfo Interface. Different from the proactive *TX payer*, the role *observer* is designed for analyzing the received block information sent from consensus nodes. With the dedicated interface *HandleBlockInfo*, the *observer* can take advantage of the block information. For instance, when *BlockEmulator* emulates an algorithm of account redistribution, *observer* needs to generate an account graph exploiting the TXs collected from the previous epoch. This account graph is then used for the generation of account-partition results.

Users can also design how to measure their metrics using the interface *HandleBlockInfo*. By implementing the interface *HandleBlockInfo*, users can define customized functionalities to measure their interested metrics.

To achieve the goal of metric measuring, three functions should be redefined within the interface *HandleBlockInfo*, including a constructor function for data structure, a metric-updating function, and a result-output function. At the system’s initialization stage, a dedicated data structure specified by this interface is created. Then, this data structure is designed to process and store metric-related information. Upon receiving block messages from worker nodes, the *observer* automatically updates this data structure following the metric-updating function. When the system terminates, the *observer* invokes the result-output function to calculate the final metrics using the data structure and subsequently outputs the results to disk. Thus, this customizable interface can enable users to collect and manage experimental results conveniently.

D. Other Featured Implementations

1) *Implementation of Account Redistribution*: In Section III-B, we discussed CLPA algorithm [15]. The *Main* shard generates an account graph based on blocks collected from an epoch and runs CLPA on the graph when the current epoch expires.

We implement CLPA in *BlockEmulator* and separate the graph-related functions from the consensus layer. Users can thus invoke CLPA even in a non-blockchain environment. We also prune CLPA results to reduce their sizes. Accounts are called *dirty* ones if they need to migrate, and only these accounts will be included in the result of account redistribution.

To reduce the communication overhead among nodes, *BlockEmulator* recruits *observer* nodes as the members of the *Main* shard. In our demonstration code, we implement the CLPA graph-generation function and the execution of the CLPA redistribution algorithm in interfaces *HandleBlockInfo* and *MsgSendingControl*, respectively. The interface *HandleBlockInfo* will be triggered by the block information message sent from the *workers*. This mechanism facilitates the on-going generation of the CLPA graph according to the arrived new blocks. When the conditions for reconfiguration are met, e.g., a predetermined time interval or a specified number of transactions have been processed, the interface *MsgSendingControl* will be invoked. This triggers the execution of the CLPA redistribution algorithm, and the results are subsequently disseminated to *worker* shards.

2) *Implementation of Account Migration*: When receiving the result of account redistribution, *worker* shards need to save the result and perform account migration. To enable this, the interfaces *ExtraOpInConsensus* and *OpInterShards* should be rewritten carefully.

BlockEmulator adopts a lock-based mechanism to implement the account migration. Once the leader node of a *worker* shard receives the command of account redistribution, it completes the current round of PBFT first, then locks the associated account states in this shard. After these prepara-

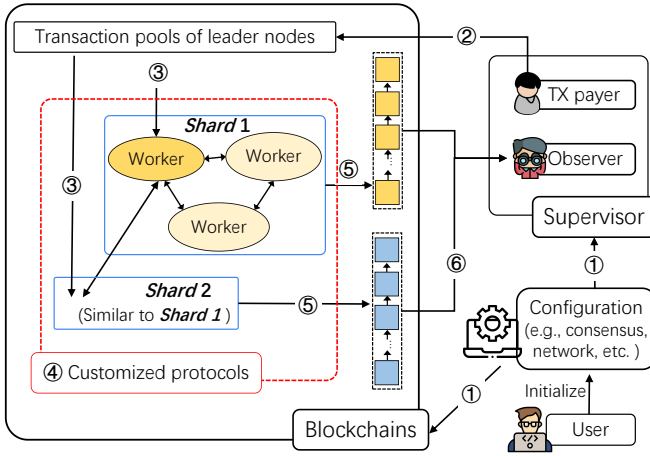


Fig. 6: The workflow of BlockEmulator. The six steps when using BlockEmulator are explained as follows: ① : Developers set up the configuration of blockchains and the supervisor. ② : The supervisor injects transactions. ③ : Leaders load transactions from the pool. ④ : Worker nodes operate according to customized protocols. ⑤ : All worker nodes commit blocks on the chain, update the state tree, and store data locally. ⑥ : Worker nodes send block information to the supervisor.

tions, the leader node will handle the account-migration command. Thus, the interface *ExtraOpInConsensus* should handle the message containing the account redistribution result. By implementing this interface, the leader node determines which account information should be sent to a new designated shard. The information includes account states and the transactions associated with *dirty* accounts.

A shard will unlock its account states when receiving all the *dirty* account information from other shards. Then, this shard executes the consensus of the account migration, which can be seamlessly achieved by modifying the interface *OpInterShards*. Note that, users can define a new block type dedicated to account migration. This approach ensures the compatibility of the codebase while facilitating the implementation of customized functionalities. Users can also replace the account migration module according to their demands.

The aforementioned examples indicate that users can customize their protocols or algorithms utilizing the provided interfaces. However, users should notice the following reminders. First, users must clearly define which nodes execute what functions, and where to implement their customized functionalities in either a *worker* or a *supervisor* node. Second, users should determine the timing of function execution, which will affect which interfaces should be rewritten. Finally, users need to implement the core components of their customized protocol.

E. Workflow of BlockEmulator

BlockEmulator works following the workflow (i.e., Fig. 6), where we take PBFT as an illustrative intra-shard consensus.

- In step ①, before the BlockEmulator system gets started, users/developers set up the configuration parameters for the emulated blockchain. The configuration parameters

mainly include the directory of the output of experimental results, block-generation interval, the consensus protocol adopted, block size, the number of nodes per shard, and the total number of blockchain shards across the network, etc. Then, the BlockEmulator system generates a blockchain according to the configured parameters. When employing PBFT, a *leader* node will be elected for each shard, followed by initializing all *worker* nodes.

- In step ②, the *supervisor* node simulates the role of *TX payers*. It continuously loads transactions from a local dataset and injects them into the TX pool of each shard at a pre-defined static or dynamic rate. Both the dataset's directory and the transaction injection rate are configurable parameters in the system.
- Subsequently, in step ③, the *leader* node of each shard begins to manage a set of incoming transactions received from the *supervisor*. These transactions are selected for inclusion in the newly generated block. The transaction selection mechanism employed by the *leader* is governed by predefined criteria, which could be a strategy maximizing fee revenue by prioritizing transactions by their fees, or a first-in-first-out (FIFO) ordering policy.
- In step ④, *worker* nodes operate according to user-specified customized protocols, which include both inner-shard and inter-shard protocols. The methods defined in the *ExtraOpInConsensus* interface are invoked when nodes handle inner-shard consensus. Taking PBFT as an example, after the *leader* node selects a set of transactions and packages them into a new block, the method *op_mining* in the *ExtraOpInConsensus* interface will be invoked (in the *pre-prepare* phase). This block is considered a PBFT proposal and is then proposed by the *leader* node within its shard. During the PBFT consensus, the method *op_verification* is triggered when a node receives a block from another node (e.g., in the *prepare* phase of PBFT). The method *op_confirmation* is then invoked when a node commits a block (e.g., in the *commit* phase of PBFT). These methods build up the logic of consensus in each shard's blockchain. They mitigate the risk of erroneous or malicious blocks being committed to the ledger.
- When an operation requires information from other shards, nodes engage in inter-shard communication. This communication serves various inter-shard events, such as cross-shard transaction verification, cross-shard account migrations, and transaction-proof deliveries. As depicted in Fig. 5, the method *handleInterShardMsg* is defined in interface *OpInterShards*. Through customized protocols, users can define a unique message-handling logic in this method. Once receiving a message, a *worker* node extracts the message header from the raw message and subsequently delivers the message to the appropriate function accordingly. For instance, when a node receives a CTX message, it determines the type of the message and then routes it to the appropriate function responsible for handling CTX messages. This function validates the correctness of the CTXs and appends them to the TX pool.

- When *worker* nodes achieve consensus through PBFT in step ④, each node proceeds to append the block to the blockchain in step ⑤. During step ⑤, the nodes also update the state trie and perform persistent storage of the block on local disk.
- Throughout the execution of the emulated blockchain, the *supervisor* serves as the role of an *observer*. It continuously monitors the operations and information across the entire blockchain, and updates metric data as outlined in step ⑥. By implementing the interface *HandleBlockInfo*, the *supervisor* aggregates shard information from all shards. This allows the *supervisor* to analyze the system’s performance from multiple aspects, including transactions per second, transaction confirmation latency, transaction distributions, etc.

The metric data and block information collected by the supervisor are stored in the local disk for experimental analysis.

F. In-depth Discussion

State Machine Replication. BlockEmulator achieves complete state machine replication at each node while implementing the PBFT protocol. During operation, the Merkle root of the state trie is output. By comparing the Merkle roots of the state tries across different nodes within the same shard, users can verify the consistency of these Merkle roots. Each node executes the identical PBFT consensus protocol, ensuring this comparison is meaningful. This consistency confirms that the platform successfully realizes complete state machine replication across all nodes within a shard. Furthermore, nodes will classify a block as invalid if the Merkle root contained within that block does not align with the local Merkle root.

View-change in PBFT. View-change operation is a secure mechanism in PBFT. To implement this, we set a timer for each node. When a block is committed, the timer resets and starts counting down again. If the nodes within a shard fail to reach consensus, the timer will count to zero. At that point, these nodes will initiate a view-change proposal to change the leader of the PBFT consensus, thereby ensuring the liveness of the blockchain. Users can adjust the timeout threshold that activates the PBFT view-change mechanism by configuring the `PbftViewChangeTimeOut` parameter. The implementation code of the view-change mechanism can be found from our open-source GitHub project¹.

V. EXPERIMENTS AND ANALYSIS

This section shows comprehensive measurements and tests to prove that BlockEmulator is useful and can produce correct emulation results.

A. Performance Metrics to Verify BlockEmulator

When analyzing the functional performance of *BlockEmulator*, we mainly focus on four metrics, including *transactions per second* (TPS) [26], *transaction confirmation latency* (TCL) [17], *cross-shard transaction ratio* (CTX Ratio) [27],

¹https://github.com/HuangLab-SYSU/block-emulator/blob/main/consensus_shard/pbft_all/view_change.go

TABLE II: Symbols used in experimental settings.

Θ	Size of a block
δ	Interval between two blocks (second)
\mathcal{R}	The set of transactions handled
N	Number of shards
t	Time cost in the phase
ϕ	The speed of transaction packing
$\mathbb{E}'(\text{TPS})$	TPS expectation for a single shard
$\mathbb{E}(\text{TPS})$	TPS expectation for the whole system
TCL_z	TCL expectation for regular TXs
TCL_y	TCL expectation for cross-shard TXs

and *TX pool size*. A more detailed description of each metric is as follows.

- **TPS** is applied to measure the ability of transaction handling of a blockchain system. Note that, a cross-shard transaction is deemed confirmed if its *intra-shard* and *inter-shard* relay transactions are both on-chain. Thus, we count an intra-shard relay transaction or an inter-shard relay transaction as 0.5 in our calculation method for TPS.
- **TCL** is the interval counted from the timeslot when a transaction is proposed to the timeslot when this transaction is confirmed. In the context of blockchain, it refers to the time consumed between when a transaction is broadcasted to the network and when it is included in a block and confirmed by the network.
- **CTX Ratio** refers to the proportion of transactions whose payer and payee accounts are located in different shards out of the total number of transactions submitted to TX pools. A transaction requires less overhead for message propagation and storage if its payer and payee accounts are located in the same shard. A higher CTX Ratio might lead to longer latency and lower throughput.
- **TX pool size** stands for the length of the TX pool queue. It can not only reflect real-time changes in the TX pool but also indicate the transaction workload of each shard.

B. Experimental Settings

In the following experiments, a block can maintain a maximum of 2,000 transactions. The interval between two blocks in each shard is set to 8 seconds. Each epoch lasts for 80 seconds. These settings allow users to analyze the system’s performance in different epochs. The experiments are conducted on 10 resource-heterogeneous physical machines configured with the Ubuntu 20.04.6LTS operating system. The hardware configurations of those physical machines are 5 Xeon(R) W-2150B CPU and 64 GB RAM, 3 Inte(R) Core(TM) i7-9700F CPU and 64GB RAM, 1 Inte(R) Core(TM) i7-9700F CPU and 16 GB RAM, and 1 AMD Ryzen 9 3900x 12-core CPU and 16 GB RAM. Moreover, multiple shards are deployed on each physical machine. Most modules of *BlockEmulator* are implemented using the Go language. Please find the open-source implementation from our GitHub project [18].

Datasets. The experiments utilize both a randomly generated synthetic dataset and a historical Ethereum dataset.

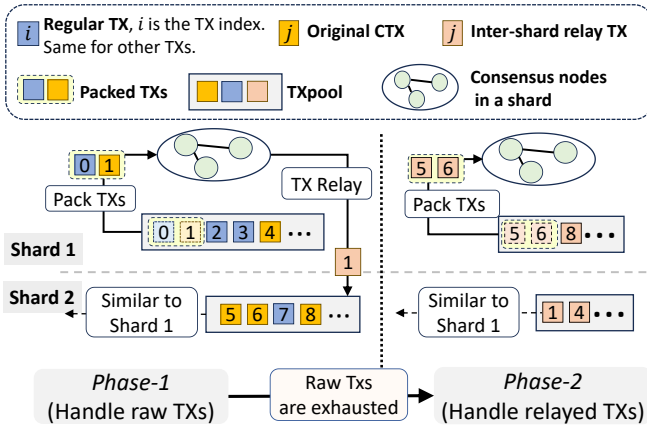


Fig. 7: Correctness demonstration of the TX pools in Phase-1 and Phase-2. These two phases are defined to help understand the evolution of TX pools if given a group of injected raw transactions.

Dataset i) The synthetic dataset, comprising load-balanced transactions, is used to verify the correctness of *BlockEmulator*. *Dataset ii)* The historical dataset, sourced from the Ethereum blockchain [28], includes real-world transactions (excluding smart contract interactions) from block heights 2,000,000 to 2,999,999.

Launching BlockEmulator. Through modifying parameter configurations and IP-address files, we then use a pre-compiled executable code to generate batch command files for each shard. Next, we can launch all nodes to run *BlockEmulator*. The guidance manual for launching *BlockEmulator* is available in our GitHub project [18].

C. Correctness Verification of BlockEmulator's Observed Results

To demonstrate the correctness of *BlockEmulator*, we conduct this group of experiments at a high scale. We evaluate the TPS and TCL versus different numbers of shards. We also set the total number of transactions \mathcal{W} to $100,000 \times N$, where N is the number of shards in each group of experiments. Therefore, the system runs for a sufficiently long time under different settings of N .

For a more detailed validation, we first utilize a manual dataset to generate load-balanced transactions randomly across all shards. We also configure the transaction fees so that the priorities of transactions are equal in TX pools. The TX pool of each shard thus becomes a FIFO queue. To mitigate the impact of transaction injection, the nodes collect all transactions and put them into TX pools before the consensus starts. In addition, the system adopts the *Relay* mechanism [16] to process cross-shard transactions and applies a static sharding algorithm. Finally, we calculate the expected performance of TPS in all the 3 phases of transaction handling and analyze the distributions of TCL for both regular transactions and cross-shard transactions. We then compare the experimental results obtained from *BlockEmulator* with the theoretical computations.

1) Mathematical Analysis:

Expected Performance of TPS in 3 TX-handling Phases.

Each shard begins to handle inter-shard relay transactions until all the regular and intra-shard relay transactions are handled in the TX pool. This is because the TX pool is a FIFO queue, and all transactions are collected before the system starts to run. Thus, the following 3 phases of TX handling are depicted as follows. *i)* Phase-1, during which the system processes only raw transactions and adds derived inter-shard relay TXs to the TX pools. *ii)* Phase-2, where only inter-shard relay TXs are processed. *iii)* Phase-3, representing the combined duration of both Phase-1 and Phase-2. The evolution of TX pools in Phase-1 and Phase-2 are shown in Fig. 7. Initially, the system is in Phase-1, and the TX pools comprise only raw TXs, i.e., regular TXs and original CTXs. Once all raw TXs in the pools have been processed and exhausted, the system shifts from Phase-1 to Phase-2. At this stage, the TX pool exclusively contains inter-shard relay TXs.

The relevant symbols and explanations are provided in Tab. II. The equation $\mathbb{E}(\text{TPS}) = \mathbb{E}'(\text{TPS}) \times N$ holds due to the balanced workloads of all shards. We can derive from Eq.(1) that $|\mathcal{U}| = |\mathcal{V}| = |\mathcal{Y}| = \frac{N-1}{N} \cdot |\mathcal{X}|$, $|\mathcal{Z}| = \frac{1}{N} \cdot |\mathcal{X}|$. We can also calculate the speed of transaction packing: $\phi = \Theta \cdot N/\delta$.

Then, let $\mathbb{E}_1(\text{TPS})$, t_1 , \mathcal{R}_1 and \mathcal{W}_1 denote $\mathbb{E}(\text{TPS})$, t , \mathcal{R} and \mathcal{W} in Phase-1, respectively. Similar symbols apply to the other 2 phases. The mathematical expectations of TPS of these 3 phases are provided as follows.

- **Phase-1.** In this phase, the system packs both regular and intra-shard relay transactions into blocks, since inter-shard relay transactions are at the end of the TX pool queues. According to the $|\mathcal{V}|$ and $|\mathcal{Z}|$, we can get $|\mathcal{R}_1| = |\mathcal{V}|/2 + |\mathcal{Z}| = \frac{N+1}{2N} \cdot |\mathcal{X}|$, and $|\mathcal{W}_1| = |\mathcal{V}| + |\mathcal{Z}| = |\mathcal{X}|$. The expectation time cost t_1 can be calculated as dividing $|\mathcal{W}_1|$ by the transaction packing speed ϕ . Thus, we have $t_1 = |\mathcal{W}_1|/\phi = \frac{\delta \cdot |\mathcal{X}|}{\Theta \cdot N}$. Therefore, the TPS expectation for Phase-1 is expressed as:

$$\mathbb{E}_1(\text{TPS}) = |\mathcal{R}_1|/t_1 = \frac{\Theta \cdot (N+1)}{2\delta}. \quad (3)$$

- **Phase-2.** In this phase, the system handles the inter-shard relay transactions only. A block packs a number Θ of transactions but the credit is only $\Theta/2$. Thus, $\mathbb{E}_2(\text{TPS})$ can be calculated by dividing the speed of transaction packing by 2:

$$\mathbb{E}_2(\text{TPS}) = \phi/2 = \frac{\Theta \cdot N}{2\delta}. \quad (4)$$

- **Phase-3.** In the whole TX execution combined phase-1 and phase-2, the number of transactions the system packs is $|\mathcal{W}_3| = |\mathcal{Z}| + |\mathcal{U}| + |\mathcal{V}| = \frac{2N-1}{N} \cdot |\mathcal{X}|$. Here, t_3 is the time cost by packing these $|\mathcal{W}_3|$ transactions on the chain, and it can be calculated like that in Phase-1: $t_3 = |\mathcal{W}_3|/\phi = \frac{\delta \cdot (2N-1) \cdot |\mathcal{X}|}{N^2 \cdot \Theta}$. Therefore, the TPS expectation in Phase-3 is written as follows:

$$\begin{aligned} \mathbb{E}_3(\text{TPS}) &= |\mathcal{R}_3|/t_3 = |\mathcal{X}|/t_3 \\ &= \frac{N^2 \cdot \Theta}{2\delta}. \end{aligned} \quad (5)$$

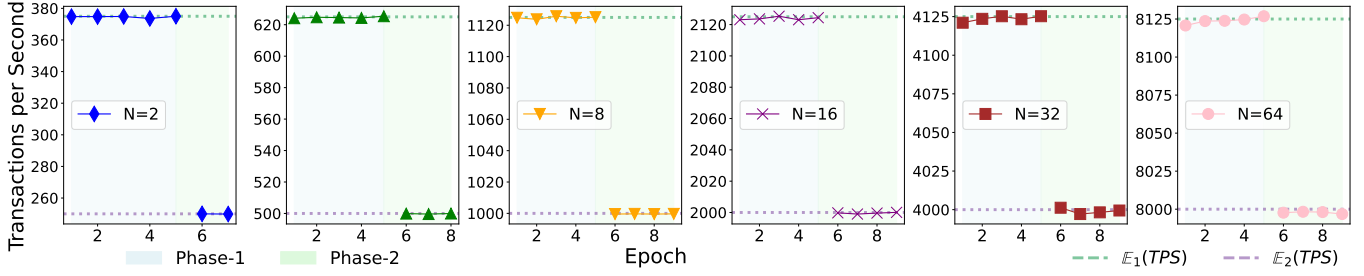
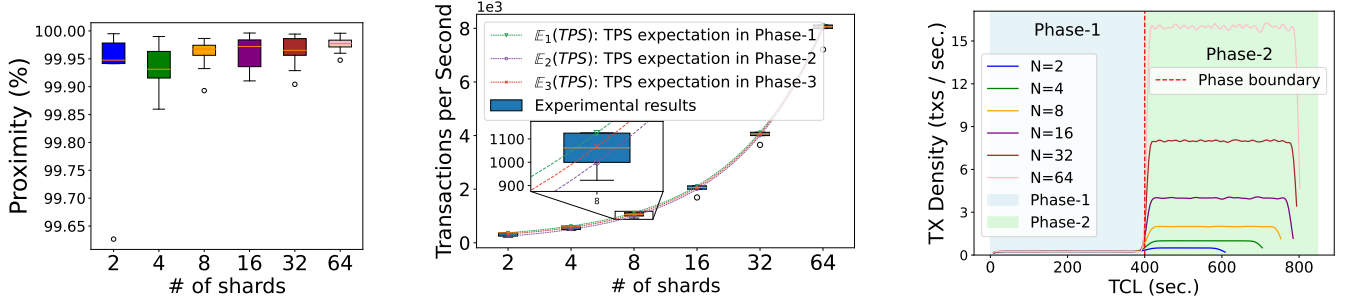


Fig. 8: Comparison of the theoretical and experimental results in terms of TPS. The two horizontal dashed lines in each figure represent the $\mathbb{E}_1(\text{TPS})$ and $\mathbb{E}_2(\text{TPS})$ in the corresponding setting of shard numbers.



(a) The proximity (measured in percentage) between the experimental results and expectations.

(b) Comparison of the theoretical expectations on TPS and experimental results in the 3 phases of TX handling.

(c) TCL distributions vs different shard numbers. The raw TXs are exhausted and the system shifts to Phase-2 at the *phase boundary*.

Fig. 9: Correctness verification. The comparison of experimental performance and theoretical derivation, with respect to the expected TPS and TCL distribution across different TX-handling phases.

Distributions of TCL for Regular TXs and Cross-shard TXs. Before the system begins processing TXs, due to random generation, both regular TXs and cross-shard TXs in the TX pools are uniformly distributed. We reuse the previously mentioned Phase-1 and Phase-2 to explain the evolution of all transactions in TX pools.

In Phase-1, nodes pack both regular TXs and cross-shard TXs. If a cross-shard TX is packed as an intra-shard relay TX, a corresponding inter-shard relay TX will be sent to another destined shard and appended to the end of that shard's TX pool queue. Therefore, only regular TXs are handled thoroughly in Phase-1. In Phase-2, only inter-shard relay TXs are left in TX pools. In other words, only cross-shard TXs are handled in Phase-2.

Given that the TX pools are FIFO queues and the TX packing speed is a constant ϕ , the transaction confirmation latency (TCL) for both types of transactions are distributed uniformly. In detail, the TCL distributions of these two types of TXs are calculated as follows.

- **The TCL distribution of regular TXs.** Initially, the mathematical expected number of TXs in all TX pools is \mathcal{W} . The expected time duration of Phase-1 is $\frac{\mathcal{W}}{\phi}$. Recall that $\phi = \Theta \cdot N/\delta$, the duration can be written as $\frac{\mathcal{W} \cdot \delta}{N \cdot \Theta}$. As mentioned before, each shard handles regular TXs in Phase-1. Because of the random generation for TXs, the TCL of regular TXs $\text{TCL}_{\mathcal{Z}}$ follows a uniform distribution. Thus, we have $\text{TCL}_{\mathcal{Z}} \sim \text{Uniform}(0, \frac{\mathcal{W} \cdot \delta}{N \cdot \Theta})$.

- **The TCL distribution of cross-shard TXs.** As mathematical expectation, there are a number $\frac{(N-1) \cdot \mathcal{W}}{N}$ of cross-shard TXs being handled in Phase-2. The expected time duration of Phase-2 is $\frac{\mathcal{W} \cdot (N-1)}{\phi \cdot N}$. Therefore, the TCL of cross-shard $\text{TCL}_{\mathcal{Y}}$ follows a uniform distribution, i.e., $\text{TCL}_{\mathcal{Y}} \sim \text{Uniform}(\frac{\mathcal{W} \cdot \delta}{N \cdot \Theta}, \frac{\mathcal{W} \cdot \delta}{N \cdot \Theta} + \frac{\mathcal{W} \cdot \delta \cdot (N-1)}{\Theta \cdot N^2})$.

Since TXs are generated randomly and uniformly, the derived results indicate that the distributions of TCL for both regular TXs and cross-shard TXs follow uniform distributions. If TXs are non-uniformly generated or exhibit bias, the TCL distribution will also vary accordingly.

2) *Experiment results and comparisons:* Fig.8 shows the piecewise TPS for each epoch when the number of shards varies. The two dashed lines in this figure refer to $\mathbb{E}_1(\text{TPS})$ and $\mathbb{E}_2(\text{TPS})$, i.e., the TPS expectations for Phase-1 and Phase-2, respectively. The TPS curves stabilize around the $\mathbb{E}_1(\text{TPS})$ and $\mathbb{E}_2(\text{TPS})$ lines during Phase-1 and Phase-2, respectively. These findings confirm that the results of the experiments are as expected.

Fig.9(a) illustrates the proximity percentages between the observed TPS of each epoch and the expected TPS versus varying shard numbers. The results demonstrate that the observed experimental values closely align with the theoretical expectations for each shard configuration. Fig. 9(b) presents the experimental TPS for each epoch alongside the phase-wise TPS expectations. In the magnified subplot, the $\mathbb{E}_1(\text{TPS})$ curve aligns with the upper quartile, while the $\mathbb{E}_2(\text{TPS})$ curve

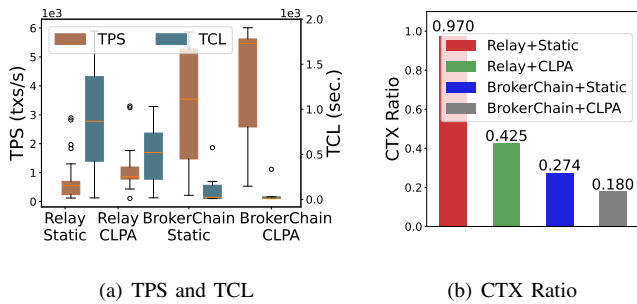


Fig. 10: Evaluation on TPS, TCL, and CTX Ratio while invoking 4 mechanisms, i.e., Relay+Static, Relay+CLPA, BrokerChain+Static, and BrokerChain+CLPA.

matches the lower quartile of the box plot. The $\mathbb{E}_3(\text{TPS})$ curve crosses between these two.

TCL distributions are shown in Fig. 9(c). Note that the total # of TXs is $\mathcal{W} = 100,000 \times N$. Thus, the vertical red dashed line *phase boundary* is fixed at $\text{TCL} = \frac{\mathcal{W} \cdot \delta}{N \cdot \Theta} = 400^{\text{th}}$ second for all shard number configurations. To the left of the *phase boundary* line, the system is in Phase-1 and only packages raw TXs. To the right of this line, the system works in Phase-2 and exclusively packages inter-shard relayed TXs. The observation demonstrates that the TCL follows a uniform distribution in both Phase-1 and Phase-2, which aligns with our theoretical analysis.

D. Various Metrics Supported to Measure

To show adequate performance testing functionalities of *BlockEmulator*, we conduct another group of experiments, in which approximately 1.6 million historical transactions of Ethereum [28] were adopted as the dataset. The number of shards is set to 32 and the number of nodes in each shard is set to 4. In other words, we run 128 nodes in our physical machines. In addition, we fix the transaction injection rate with 4,000 txs/s by default and increase it by 4,000 txs/s each the next epoch.

To reveal the features of supporting secondary development, we also implement some state-of-the-art mechanisms in our *BlockEmulator* and compare them using different metrics. The mechanisms we have implemented are introduced as follows.

- **Relay+Static.** The system handles cross-shard transactions with *transaction relay mechanism* [16]. The account states are divided into different shards by a static sharding method.
- **Relay+CLPA.** The cross-shard transaction handling method is *transaction relay mechanism*. The account states are redistributed using CLPA [15], which is a dynamic sharding algorithm.
- **BrokerChain+Static.** BrokerChain protocol [17] is adopted to handle cross-shard transactions. The account states are sharded statically.
- **BrokerChain+CLPA.** This mechanism integrates the solutions of broker accounts and CLPA.

In our experiments, we selected the top 10 accounts that transfer the most transactions as broker accounts. The transactions in which these broker accounts are involved have

a proportion of 80% of total transactions. With these well-selected broker accounts, the BrokerChain-related mechanisms thus perform better. We use an offline-version CLPA algorithm on partial data and find that the CTX Ratio is reduced by about 55%. Therefore, we expect that *BrokerChain+Static* will outperform *Relay+CLPA*, and *BrokerChain+CLPA* will show better performance than *BrokerChain+Static*.

As depicted in Fig. 10(a), *BrokerChain+Static* outperforms *Relay+CLPA*, and both of them perform better than *Relay+Static* in terms of TPS and TCL. The results of this group of experiments perfectly match what we predicted in the previous paragraph.

Interestingly, *BrokerChain+CLPA* does not show a dominating advantage than *BrokerChain+Static*. One possible reason is that the *CLPA* algorithm requires a reconfiguration stage for account migration, resulting in additional time consumption. Another reason can be inferred from Fig. 10(b), in which it implies that *Relay+CLPA* has a much lower CTX ratio than *Relay+Static*. However, *BrokerChain+CLPA* has a slightly lower CTX ratio than *BrokerChain+Static*. This means that *BrokerChain* mechanism has already significantly reduced the CTX Ratio, and the impact of running *CLPA* is thus not apparent.

Fig. 11(a) shows that the accumulative size of TX pools varies over time. Note that, in mechanisms *BrokerChain+CLPA* and *Relay+CLPA*, TX pool size suddenly descends and rises at some timeslots. This is because the transaction mitigation operations in *CLPA*. In addition, the TX pool size performance of both *BrokerChain+Static* and *BrokerChain+CLPA* increases slowly but declines fast. This observation indicates that these two mechanisms yield higher TPS and fewer accumulated transactions in TX pools compared to the other two mechanisms.

To further explore why *BrokerChain+CLPA* and *BrokerChain+Static* perform better in Fig. 11(a), we evaluate the workload distribution across shards. The observed results are shown in Fig. 11(b). The workload of each shard is calculated by summing up the packed transactions in all committed blocks within the shard. *BrokerChain+CLPA* shows the most balanced workloads because its CDF curve rises rapidly. This observation indicates a high density of workload percentages, which suggests balanced workloads across shards. The CDF curve of *Relay+Static* grows slowly, while the CDFs of the other 3 mechanisms reach 1.0 fast. This observation shows that both *CLPA* and *BrokerChain* are effective when balancing workloads.

From Fig. 11(a), we find that the curves of *Relay+CLPA* and *Relay+Static* are close for the first 200 seconds. The curves of *BrokerChain+CLPA* and *BrokerChain+Static* show almost the same. These observations are interesting. Thus, we conducted another experiment to find some clues. This group of experiments runs for 1000 seconds. We record TPS every epoch (i.e., 80 seconds). To get adequate experimental data, we use about 8 million historical transactions collected from Ethereum [28].

Fig. 11(c) demonstrates the TPS of the 4 mechanisms at different transaction injection rates. Surprisingly, *CLPA* has few or negative effects while integrating with *Relay* and

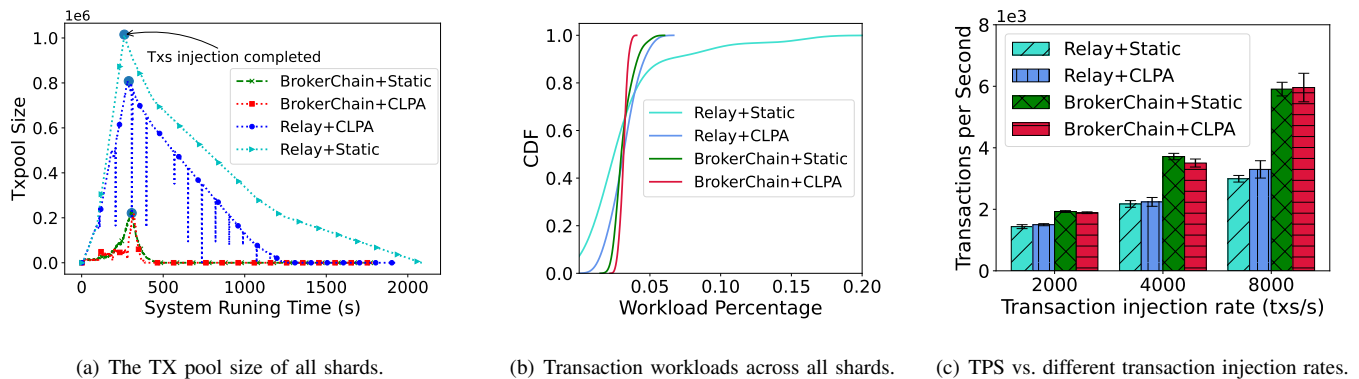


Fig. 11: Evaluation on time-varying TX pool size, workloads, and TPS vs. different TX injection rates.

Brokerchain mechanisms. This is because *CLPA* improves TPS by moving transactions from the overloaded shards to the underloaded ones. However, there is almost no overloaded shard when the transaction injection rate is low. Similarly, there is almost no underloaded shard when the transaction injection rate is high. In addition, the reconfiguration time consumed by *CLPA* also leads to degradation of performance. Therefore, *CLPA* performs better if the transaction injection rate is low and TX pools are full. In Fig. 11(a), *CLPA* outperforms when transaction injection stops. This observation confirms our aforementioned explanation.

Finally, when the transaction injection rates are relatively low, the TPS of *BrokerChain+CLPA* and *BrokerChain+Static* are very close to the injection rates. This is because *BrokerChain* can shift a cross-shard transaction to a regular transaction if its payer or payee is a broker account. The proper broker accounts we selected for experiments help these two *BrokerChain*-related mechanisms work well.

VI. CONCLUSION

BlockEmulator is designed as a testbed for blockchain researchers. It not only supports some basic operations in existing blockchains but also offers powerful programming interfaces for evaluating new blockchain protocols or consensus algorithms. In particular, it enables researchers to develop and evaluate new customized blockchain-sharding protocols. To verify the correctness of the experiment data yielded by BlockEmulator, we conducted experiments to compare the observed performance with the theoretical calculation. Other experiments prove that BlockEmulator supports meaningful performance testing in terms of typical metrics in a blockchain sharding system, including TPS, transaction confirmation latency, cross-shard transaction ratio, and the queuing length of transaction pools.

We have made open-sourced BlockEmulator in Github [18]. This project has been starred over 210 times and forked 60 times. We wish BlockEmulator could become a practical and useful experimental tool for blockchain researchers when they need to implement and test new protocols, algorithms, and mechanisms.

ACKNOWLEDGEMENTS

We appreciate all the great efforts made by the students who graduated from HuangLab, such as Xiaowen Peng, Jianzhou Zhan, Shenyang Zhang, Canlin Li, Yue Lin, Yetong Zhao, and other team members who are not shown in the author list, including Miaoyong Xu, Junhao Wu, and Jian Zheng.

REFERENCES

- [1] T. T. A. Dinh, J. Wang, G. Chen, R. Liu, B. C. Ooi, and K.-L. Tan, "Blockbench: A framework for analyzing private blockchains," in *Proc. of the 2017 ACM international conference on management of data*, 2017, pp. 1085–1100.
- [2] L. Stoykov, K. Zhang, and H.-A. Jacobsen, "Vibes: fast blockchain simulations for large-scale peer-to-peer networks," in *Proc. of the 18th ACM/IFIP/USENIX Middleware Conference: Posters and Demos*, 2017, pp. 19–20.
- [3] Y. Aoki, K. Otsuki, T. Kaneko, R. Banno, and K. Shudo, "Simblock: A blockchain network simulator," in *Proc. of IEEE Conference on Computer Communications Workshops (INFOCOM WKSHPs)*. IEEE, 2019, pp. 325–329.
- [4] D. Mohanty and D. Mohanty, "Deploying smart contracts," *Ethereum for Architects and Developers: With Case Studies and Code Samples in Solidity*, pp. 105–138, 2018.
- [5] N. Prusty, *Building blockchain projects*. Packt Publishing Ltd, 2017.
- [6] OpenEthereum, "The Fastest and most Advanced Ethereum Client." <https://github.com/openethereum/parity-ethereum>, Retrieved: May 23, 2023.
- [7] E. Androulaki, A. Barger, V. Bortnikov, C. Cachin, K. Christidis, A. De Caro, D. Enyeart, C. Ferris, G. Laventman, Y. Manevich, *et al.*, "Hyperledger fabric: a distributed operating system for permissioned blockchains," in *Proc. of the thirteenth EuroSys conference (EuroSys)*, 2018, pp. 1–15.
- [8] R. G. Brown, "The corda platform: An introduction," *Retrieved*, vol. 27, p. 2018, 2018.
- [9] M. Li, Y. Lin, J. Zhang, and W. Wang, "CoChain: High Concurrency Blockchain Sharding via Consensus on Consensus," in *IEEE INFOCOM 2023-IEEE Conference on Computer Communications*. IEEE, 2023, pp. 1–10.
- [10] M. Li, W. Wang, and J. Zhang, "LB-Chain: Load-Balanced and Low-Latency Blockchain Sharding via Account Migration," *IEEE Transactions on Parallel and Distributed Systems*, 2023.
- [11] Z. Hong, S. Guo, E. Zhou, W. Chen, H. Huang, and A. Zomaya, "GridB: Scaling Blockchain Database via Sharding and Off-Chain Cross-Shard Mechanism," *Proceedings of the VLDB Endowment*, vol. 16, no. 7, pp. 1685–1698, 2023.
- [12] G. Wood *et al.*, "Ethereum: A secure decentralised generalised transaction ledger," *Ethereum project yellow paper*, vol. 151, no. 2014, pp. 1–32, 2014.
- [13] X. Qi, "S-Store: A Scalable Data Store towards Permissioned Blockchain Sharding," in *Proc. of IEEE Conference on Computer Communications (INFOCOM)*. IEEE, 2022, pp. 1978–1987.

- [14] L. Yang, S. J. Park, M. Alizadeh, S. Kannan, and D. Tse, "DisperseDLedger: High-Throughput Byzantine Consensus on Variable Bandwidth Networks," in *Proc. of 19th USENIX Symposium on Networked Systems Design and Implementation*, 2022, pp. 493–512.
- [15] C. Li, H. Huang, Y. Zhao, X. Peng, R. Yang, Z. Zheng, and S. Guo, "Achieving Scalability and Load Balance across Blockchain Shards for State Sharding," in *Proc. of 2022 41st International Symposium on Reliable Distributed Systems (SRDS)*. IEEE, 2022, pp. 284–294.
- [16] J. Wang and H. Wang, "Monoxide: Scale out blockchains with asynchronous consensus zones," in *Proc. of 20th USENIX Symposium on Networked Systems Design and Implementation*, vol. 2019, 2019, pp. 95–112.
- [17] H. Huang, X. Peng, J. Zhan, S. Zhang, Y. Lin, Z. Zheng, and S. Guo, "Brokerchain: A cross-shard blockchain protocol for account/balance-based state sharding," in *Proc. of IEEE Conference on Computer Communications (INFOCOM)*, 2022, pp. 1968–1977.
- [18] "BlockEmulator." [Online]. Available: <https://github.com/HuangLab-SYSU/block-emulator>
- [19] M. Castro, B. Liskov, *et al.*, "Practical byzantine fault tolerance," in *OsDI*, vol. 99, no. 1999, 1999, pp. 173–186.
- [20] W. A. Trybulec, "Pigeon hole principle," *Journal of Formalized Mathematics*, vol. 2, no. 199, p. 0, 1990.
- [21] S. Zhang and J.-H. Lee, "Double-spending with a sybil attack in the bitcoin decentralized network," *IEEE transactions on Industrial Informatics*, vol. 15, no. 10, pp. 5715–5722, 2019.
- [22] S. Gao, Z. Li, Z. Peng, and B. Xiao, "Power adjusting and bribery racing: Novel mining attacks in the bitcoin system," in *Proc. of the 2019 ACM SIGSAC Conference on Computer and Communications Security*, 2019, pp. 833–850.
- [23] L. Luu, V. Narayanan, C. Zheng, K. Baweja, S. Gilbert, and P. Saxena, "A secure sharding protocol for open blockchains," in *Proc. of the 2016 ACM SIGSAC conference on computer and communications security*, 2016, pp. 17–30.
- [24] M. Zamani, M. Movahedi, and M. Raykova, "Rapidchain: Scaling blockchain via full sharding," in *Proc. of the 2018 ACM SIGSAC conference on computer and communications security*, 2018, pp. 931–948.
- [25] C. Dwork, M. Naor, and H. Wee, "Pebbling and proofs of work," in *Advances in Cryptology—CRYPTO 2005: 25th Annual International Cryptology Conference, Santa Barbara, California, USA, August 14–18, 2005. Proceedings 25*. Springer, 2005, pp. 37–54.
- [26] S. King and S. Nadal, "Ppcoin: Peer-to-peer crypto-currency with proof-of-stake," *self-published paper, August*, vol. 19, no. 1, 2012.
- [27] Y. Zhang, S. Pan, and J. Yu, "Txallo: Dynamic transaction allocation in sharded blockchain systems," in *Proc. of IEEE 39th International Conference on Data Engineering (ICDE)*. IEEE, 2023, pp. 721–733.
- [28] P. Zheng, Z. Zheng, J. Wu, and H.-N. Dai, "XBlock-ETH: Extracting and exploring blockchain data from Ethereum," *IEEE Open J. Comput. Soc.*, vol. 1, pp. 95–106, May 2020.



Huawei Huang (SM'22) received his Ph.D. in Computer Science and Engineering from the University of Aizu (Japan). He is an Associate Professor at the School of Software Engineering, Sun Yat-Sen University, China. His research interests mainly include blockchain systems and protocols. He has served as a guest editor for multiple special issues on blockchain at IEEE JSAC, OJ-CS, and IET Blockchain. He also served as TPC chair for blockchain conferences, such as IEEE Global Blockchain Conference, IEEE SERVICES, ICWS, BlockSys, etc. He has been

recognized in the list of the yearly World's Top 2% Scientists since 2023.



Guang Ye is currently a student pursuing his master's degree at the School of Software Engineering, Sun Yat-Sen University. His research interests mainly include Blockchain.



Qinde Chen is a Ph.D. student at the School of Software Engineering, Sun Yat-sen University. His research interests mainly include blockchain.



Zhaokang Yin is currently a student pursuing his master's degree at the School of Software Engineering, Sun Yat-Sen University. His research interests mainly include Blockchain.



Xiaofei Luo is currently a postdoctoral researcher at Sun Yat-sen University. He received his Ph.D. degree in Computer Science and Engineering from the University of Aizu in March 2023. His current research interests include blockchain, payment channel networks, and reinforcement learning. His research has been published in IEEE JSAC and other well-known international journals and conferences.



Lin Jianru is a research scientist engineer of HuangLab (a blockchain laboratory at Sun Yat-sen University). He has rich experience in the design and implementation of decentralized systems, smart contract languages, and virtual machines. He is the translator of the Chinese edition of *Designing for Scalability with Erlang/OTP*.



Taotao Li received the Ph.D. degree in cyber security from the Institute of Information Engineering, Chinese Academy of Sciences and University of Chinese Academy of Sciences, China, in 2022. He is currently a postdoc with the School of Software Engineering, Sun Yat-Sen University, Zhuhai, China. His main research interests include blockchain, Web3, and applied cryptography.



Qinglin Yang received his Ph.D. degree in Computer Science and Engineering from the University of Aizu, Japan, 2021. He has been a guest editor for a blockchain special issue at IEEE OJCS. He also served as a TPC chair for several of conferences, including blockchain and machine learning. He ever worked as a Research Fellow at Sun Yat-sen University, China. He is an assistant professor at the Cyberspace Institute of Advanced Technology, Guangzhou University, China. His current research interests include federated learning, Web3,

and blockchain.



Zibin Zheng (SM'16-F'23) received a Ph.D. degree from the Chinese University of Hong Kong, Hong Kong, in 2012. He is a Professor at the School of Software Engineering, Sun Yat-Sen University, China. His current research interests include service computing, blockchain, and cloud computing. Prof. Zheng was a recipient of the Outstanding Ph.D. Dissertation Award of the Chinese University of Hong Kong in 2012, the ACM SIGSOFT Distinguished Paper Award at ICSE in 2010, the Best Student Paper Award at ICWS2010, and the IBM Ph.D. Fellowship

Award in 2010. He served as a PC member for IEEE CLOUD, ICWS, SCC, ICSOC, and SOSE.